Thermal suppression of phase separation in condensate mixtures

Arko Roy[1,2] and D. Angom[1]

[1]*Physical Research Laboratory, Navrangpura, Ahmedabad-380009, Gujarat, India*
[2]*Indian Institute of Technology, Gandhinagar, Ahmedabad-382424, Gujarat, India*

We examine the role of thermal fluctuations in binary condensate mixtures of dilute atomic gases. In particular, we use Hartree-Fock-Bogoliubov with Popov approximation to probe the impact of non-condensate atoms to the phenomenon of phase-separation in two-component Bose-Einstein condensates. We demonstrate that, in comparison to $T = 0$, there is a suppression in the phase-separation of the binary condensates at $T \neq 0$. This arises from the interaction of the condensate atoms with the thermal cloud. We also show that, when $T \neq 0$ it is possible to distinguish the phase-separated case from miscible from the trends in the correlation function. However, this is not the case at $T = 0$.

Phase-separation in a two-component fluid is ubiquitous in nature, and the transition from miscible to immiscible phase is a quintessential example of critical phenomena. One classic example is the temperature driven phase-separation in the cyclohexane-aniline mixture [1]. It is then natural to ask what are the similarities and differences in binary mixtures of quantum fluids ? The recent experimental advances in binary Bose-Einstein condensates (BECs) of dilute atomic gases provide an ideal testbed to address such a question. In the case of binary mixtures of BECs or two-species BEC (TBEC) tuning the interaction through Feshbach resonances [2, 3] can render it miscible or immiscible. Using improved experimental techniques, TBECs have been achieved in mixtures of two different alkali atoms [4–8], or two different isotopes [2, 9, 10] and atoms of the same element in different hyperfine states [11–14] over the last decade. The remarkable feature of phase-separation in TBECs has been successfully observed in ^{85}Rb-^{87}Rb [9, 10] and ^{87}Rb-^{133}Cs [7] condensate mixtures.

The criterion for phase-separation, derived from Thomas-Fermi (TF) approximation at zero temperature [15], is that the intra-(U_{11}, U_{22}) and inter-species interaction (U_{12}) strengths, must satisfy the inequality $U_{12}^2 > U_{11}U_{22}$. However, experiments are conducted at finite temperatures, and therefore, deviations from the criterion is to be expected. Theoretical studies on effects of thermal cloud on phase-separation have been carried out for homogeneous binary Bose gases using Hartree-Fock theory [16] and large-N approximation [17]. Phase-separation of trapped binary mixtures at finite temperature has also been examined using local-density approximation [18]. In this Letter we address this issue by using Hartree-Fock-Bogoliubov theory with Popov approximation (HFB-Popov) [19] to account for the thermal fluctuations. It is a gapless formalism satisfying Hugenholtz-Pines theorem [20] and can be employed to compute the energy eigenspectra of the quasi-particle excitations of the condensates.

The method has been validated extensively in single species BEC, and we have used it in our recent works to examine the effect of quantum fluctuations in TBECs [21]. In the present work, we systematically study the role of thermal fluctuations in the phenomenon of phase-separation in trapped TBECs. Our studies reveal that at $T \neq 0$, the constituent species in the TBEC undergo phase-separation at a higher U_{12} than the value predicted based on the TF-approximation at $T = 0$. Consis-

tent with experimental observations of dual species condensate of ^{87}Rb and ^{133}Cs [7], our theoretical investigations show that even when the phase-separation condition is met, there is a sizable overlap between the two species. We attribute this to the presence of the thermal cloud, which have profound affects on the miscibility-immiscibility transition. At $T = 0$, the TBECs are coherent throughout the spatial extent of the condensate, however, when $T \neq 0$ coherence decays and is reflected in the correlation function. This implies that at $T = 0$, the miscible or immiscible phases are indistinguishable from the trends in the correlation function. But, for $T \neq 0$ the miscible-immiscible transition and the associated changes in the density profiles have a characteristic signature in the form of the correlation functions. There is a smooth cross-over between the correlations functions when the transition occurs. Interspecies Feshbach resonances of ultracold bosons have been experimentally demonstrated for Na-Rb [22], K-Rb [23] and Cs-Rb [24] mixtures, but Bose condensed mixture of Na-Rb is yet to observed experimentally. The Cs-Rb condensate mixture is a stepping stone towards the production of quantum gas of dipolar RbCs molecules, as unlike the KRb molecule, the rovibrational ground state of RbCs molecule is stable against exchange of atoms. Considering this we focus our study on the finite temperature effects in the Cs-Rb condensate mixture. Other than tuning the interspecies, it is also possible to steer the condensate mixture through the miscible-immiscible transition using intraspecies Feshbach resonance. An example is the tuning of the intraspecies interaction of ^{85}Rb in ^{85}Rb-^{87}Rb [9, 10], and for this system too, we have examined the suppression of phase-separation at $T \neq 0$ [25]. It must be emphasized that, as the background scattering length of ^{85}Rb is negative, it is possible to obtain ^{85}Rb BEC [26] only with the use of Feshbach resonance [27].

Theory — We consider a cigar shaped TBEC, where the frequencies of the harmonic trapping potential satisfy the condition $\omega_\perp \gg \omega_z$ with $\omega_x = \omega_y = \omega_\perp$. In this case, the radial excitation energies are large and assume the radial degrees of freedom are frozen for which $\hbar\omega_\perp \gg \mu_k$. So, the dynamics and hence the excitations occur only along the axial direction, z-axis, of the trap. In the mean-field regime, using HFB-Popov approximation [21, 28], a pair of coupled generalized 1D Gross-Pitaevskii (GP) equations describe the dy-

namics and density distribution of the TBEC. The combined form of the equations is

$$\hat{h}_k\phi_k + U_{kk}\left[n_{ck} + 2\tilde{n}_k\right]\phi_k + U_{12}n_{3-k}\phi_k = 0, \quad (1)$$

where $\hat{h}_k = (-\hbar^2/2m_k)\partial^2/\partial z^2 + V_k(z) - \mu_k$ is the one-body part of the Hamiltonian, with $k = 1,2$ as the species label. The strength of the coupling constants are given by $U_{kk} = (a_{kk}\lambda)/m_k$ and $U_{12} = (a_{12}\lambda)/(2m_{12})$, where, for cigar shaped traps $\lambda = \omega_\perp/\omega_z \gg 1$. Without loss of generality, for stable configurations the intra-species scattering lengths a_{kk}, and the inter-species scattering length a_{12} are considered as positive (repulsive). Under the HFB approximation, the Bose field operators are decomposed as $\hat{\Psi}_k = \phi_k + \tilde{\psi}_k$, where the ϕ_ks are the stationary solutions of Eq. (1) obtained by evolving the solution in imaginary time, with $n_{ck}(z) \equiv |\phi_k(z)|^2$. The field operator $\tilde{\psi}_k(z)$ represents the fluctuation part of $\hat{\Psi}_k(z)$, it incorporates both the quantum and thermal fluctuations. The fluctuation operator, both quantum and thermal, are functions of the elementary excitations of the system, which solves the coupled Bogoliubov-de-Gennes equations

$$\hat{\mathcal{L}}_1 u_{1j} - U_{11}\phi_1^2 v_{1j} + U_{12}\phi_1\left(\phi_2^* u_{2j} - \phi_2 v_{2j}\right) = E_j u_{1j}, \quad (2a)$$

$$\hat{\underline{\mathcal{L}}}_1 v_{1j} + U_{11}\phi_1^{*2} u_{1j} - U_{12}\phi_1^*\left(\phi_2 v_{2j} - \phi_2^* u_{2j}\right) = E_j v_{1j}, \quad (2b)$$

$$\hat{\mathcal{L}}_2 u_{2j} - U_{22}\phi_2^2 v_{2j} + U_{12}\phi_2\left(\phi_1^* u_{1j} - \phi_1 v_{1j}\right) = E_j u_{2j}, \quad (2c)$$

$$\hat{\underline{\mathcal{L}}}_2 v_{2j} + U_{22}\phi_2^{*2} u_{2j} - U_{12}\phi_2^*\left(\phi_1 v_{1j} - \phi_1^* u_{1j}\right) = E_j v_{2j}, \quad (2d)$$

where $\hat{\mathcal{L}}_1 = \left(\hat{h}_1 + 2U_{11}n_1 + U_{12}n_2\right)$, $\hat{\mathcal{L}}_2 = \left(\hat{h}_2 + 2U_{22}n_2 + U_{12}n_1\right)$ and $\hat{\underline{\mathcal{L}}}_k = -\hat{\mathcal{L}}_k$. Here u_{kj}s and v_{kj}s are the Bogoliubov quasi-particle amplitudes corresponding to the jth energy eigenvalue. The quantities $\tilde{n}_k(z) \equiv \langle\tilde{\psi}_k^\dagger(z,t)\tilde{\psi}_k(z,t)\rangle$, and $n_k(z) = n_{ck}(z) + \tilde{n}_k(z)$ are defined as non-condensate, and total density, respectively. To solve the above eigenvalue equations, the u_{kj}s and v_{kj}s are decomposed into a linear combination of harmonic oscillator eigenstates. The order parameters ϕ_ks and the non-condensate densities $\tilde{n}_k$s are then the self-consistent solutions of the coupled Eqns. (1) and (2). The thermal components, in terms of the quasi-particle amplitudes, is

$$\tilde{n}_k = \sum_j\{[|u_{kj}|^2 + |v_{kj}|^2]N_0(E_j) + |v_{kj}|^2\}, \quad (3)$$

where, $N_0(E_j) = (e^{\beta E_j} - 1)^{-1}$ with $\beta = 1/(k_B T)$ is the Bose factor of the jth quasi-particle mode at temperature T. A more detailed description of the decomposition and derivation of the relevant equations are given else where [25]. In this Letter we examine the role of temperature in phase-separation of TBECs. For this, a measure of phase separation is the overlap integral

$$\Lambda = \frac{\left[\int n_1(z)n_2(z)dz\right]^2}{\left[\int n_1^2(z)dz\right]\left[\int n_2^2(z)dz\right]}. \quad (4)$$

Miscible phase is when $\Lambda = 1$ and signifies complete overlap of the two species, whereas the binary condensate is completely phase-separated when $\Lambda = 0$ [29].
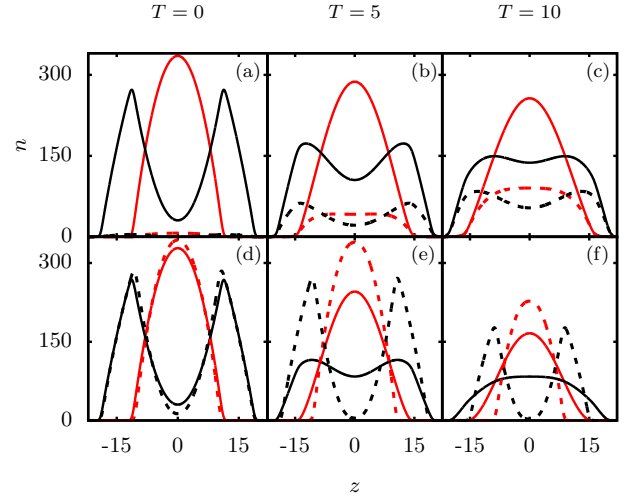

FIG. 1. (Color online) The suppression of phase-separation in ^{87}Rb-^{133}Cs TBEC at $a_{12} = 295a_0$. (a)-(c) The solid and dashed red (black) lines represent $n_{\mathrm{Cs}}(n_{\mathrm{Rb}})$ and $\tilde{n}_{\mathrm{Cs}}(\tilde{n}_{\mathrm{Rb}})$, respectively, at $T = 0,5,10$nK. (d)-(f) The solid red (black) lines represent $n_{c\mathrm{Cs}}(n_{c\mathrm{Rb}})$ at $T = 0,5,10$nK respectively. The dashed red (black) lines $n_{c\mathrm{Cs}}(n_{c\mathrm{Rb}})$ at $T = 0$ with the same number of condensate atoms at $T = 0,5,10$nK respectively. Here, n and z are measured in units of a_{osc}^{-1} and a_{osc}, respectively.

In terms of the Bose field operator $\hat{\Psi}_k$, the normalized first order or the off-diagonal correlation function, which is also a measure of the phase fluctuations, is

$$g_k^{(1)}(z,z') = \frac{\langle\hat{\Psi}_k^\dagger(z)\hat{\Psi}_k(z')\rangle}{\sqrt{\langle\hat{\Psi}_k^\dagger(z)\hat{\Psi}_k(z)\rangle\langle\hat{\Psi}_k^\dagger(z')\hat{\Psi}_k(z')\rangle}}. \quad (5)$$

It can also be expressed in terms of off-diagonal condensate and non-condensate densities as

$$g_k^{(1)}(z,z') = \frac{n_{ck}(z,z') + \tilde{n}_k(z,z')}{\sqrt{n_k(z)n_k(z')}}, \quad (6)$$

where,

$$n_{ck}(z,z') = \phi_k^*(z)\phi_k(z')$$

$$\tilde{n}_k(z,z') = \sum_j\{[u_{kj}^*(z)u_{kj}(z') + v_{kj}^*(z)v_{kj}(z')]N_0(E_j)$$
$$+ v_{kj}^*(z)v_{kj}(z')\}.$$

At $T = 0$, when the entire system is coherent and characterized by the presence of condensate only, then $g_k^{(1)} = 1$ within the extent of the condensate, whether it is in the miscible or in the immiscible regime. So, one cannot distinguish between the two phases from the nature of the correlation functions of the individual species. However, at $T \neq 0$, a clear signature of miscible-immiscible transition of the density profiles is reflected in the form of the correlation functions.

The thermal suppression of phase-separation is generic to any binary condensate mixture. However, for comparison with experimental realizations we consider the ^{133}Cs-^{87}Rb BEC mixture with ^{133}Cs labelled as species 1, and ^{87}Rb as

species 2. Here after, for brevity we drop the mass numbers and write these as Cs and Rb. The intra-species scattering lengths are $a_{11} = a_{\text{Cs}} = 280a_0$, $a_{22} = a_{\text{Rb}} = 100a_0$, the inter-species scattering length is $a_{12} = a_{\text{CsRb}} = 295a_0$ with $N_{\text{Cs}} = N_{\text{Rb}} = 5 \times 10^3$, and a_0 as the Bohr radius. To form a quasi-1D trap we take $\omega_{z(\text{Cs})} = 2\pi \times 4.55$Hz and $\omega_{z(\text{Rb})} = 2\pi \times 3.89$Hz; $\omega_{\perp(\text{Cs})} = 50\omega_{z(\text{Cs})}$ and $\omega_{\perp(\text{Rb})} = 50\omega_{z(\text{Rb})}$. For this value of $\omega_\perp$, the temperature along the radial direction is $\hbar\omega_\perp/k_B \approx 11$nK, and the tight confinement condition is valid as $\mu_k/\hbar\omega_\perp \approx 10^{-2}$. In addition to this, the healing length $\xi_k \gg 1/n_k$. Thus the system is in the weakly interacting TF regime [30] and mean field description through GP-equation is valid. For this parameter set, the ground state density distribution is phase-separated with species 1 at the center and surrounded by the species 2 at the edges. We refer to this configuration of density profiles as *sandwich* type. This choice of parameters is consistent with the experimental parameters of a recent work on quasi-1D TBEC of different hyperfine states of ^{87}Rb [31], in which dynamical evolution of mixtures of quantum gases has been observed. It should be emphasized here that *sandwich* type density profiles are applicable only to trapped systems. In uniform systems, at phase-separation, the energetically preferred states are the symmetry-broken density profiles where one species is entirely to the left and the other is entirely to the right. We refer to this configuration of density profiles as *side-by-side* type. In the present work, we demonstrate the role of thermal cloud in *sandwich* type density profiles since these are unique to trapped systems and experimentally pertinent. For the homogeneous binary condensates, using periodic boundary condition with $\omega_z = 0$ in our computations, we do get side-by-side density profiles at phase separation. As an example, the density profiles are shown in Ref. [25] and these are consistent with the results reported in previous works [32]. In the computations the spatial and temporal variables are scaled as $z/a_{\text{osc(Cs)}}$ and $\omega_{z(\text{Cs})}t$ to render the equations dimensionless.

At $T = 0$, in TBECs, as mentioned earlier, the criterion for phase separation is $U_{12} > \sqrt{U_{11}U_{22}}$. With the parameters of Cs-Rb TBEC, consider keeping a_{Cs} and a_{Rb} fixed, but varying $a_{12} = a_{\text{CsRb}}$ through a magnetic Feshbach resonance [24]. The condition for phase-separation, using TF-approximation, is then $a_{12} > 261a_0$. When $a_{12} = 0$, the TBEC is non-interacting and the two species are completely miscible, in which case $\Lambda = 1$. On increasing a_{12}, the extent of overlap between the two-species decreases, and hence Λ decreases. For instance, at $a_{12} = 50a_0$, $\Lambda = 0.97$ and it decreases monotonically with $\Lambda \to 0$ at complete phase-separation. At $a_{12} = 295a_0$, just at the onset of phase-separation, $\Lambda = 0.14$. As shown in Fig. 1(a), the density profiles corresponding to the two-species have interfacial overlap, and the interaction parameters satisfy the phase-separation condition. Furthermore, at phase separation, $n_{c\text{Cs}}(0)$ is maximum, whereas $n_{c\text{Rb}}(0) \approx 0$ and the species do not have significant overlap. In other words, Cs at the center of the trap is flanked by Rb at the edges and $\Lambda \approx 10^{-1}$. It is also to be mentioned here that for phase-separation, there is considerable difference between the values of a_{12} derived from TF approximation and the numerical solution of GP equation. This can be attributed to large gradients in condensate densities, which are ignored in the TF-approximation.
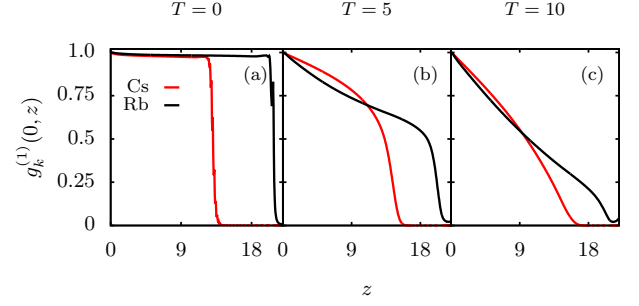

FIG. 2. (Color online) (a)-(c) The first order spatial correlation function, $g^{(1)}_{\text{Cs/Rb}}(0,z)$ with $z \geqslant 0$, of ^{87}Rb-^{133}Cs TBEC at equilibrium for $a_{12} = 295a_0$ at $T = 0, 5, 10$nK respectively. Here z is measured in units of a_{osc}.

Suppression of phase segregation — For $T \neq 0$ the Bose factor $N_0 \neq 0$, so in addition to the quantum fluctuations, the non-condensate densities $\tilde{n}_k$ have contributions from the thermal cloud as well. The condensate atoms n_{ck} then interact with $\tilde{n}_k$ of both the species, and modify n_{ck} of both the species. For illustration, at $T = 5$nK and $a_{12} = 295a_0$, the total and non-condensate density profiles are shown in Fig. 1(b). Compared to the density profiles in Fig. 1(a), there is a remarkable change in $n_{c\text{Rb}}$ as a result of the finite temperature: $n_{c\text{Rb}}(0) > 0$. Thus, keeping all the parameters same, but taking $T = 5$nK, the two species have substantial overlap as shown in Fig. 1(b) and Λ becomes ≈ 0.55. In other words, the finite temperature transforms the phase separated TBEC at $T = 0$ to a partially miscible phase. The degree of overlap increases with temperature and at $T = 10$nK, the TBEC is miscible as $\Lambda \approx 0.77$. Thus, with the increase in temperature, the density of thermal cloud increases and the *phase-separation is suppressed*. This is evident from Fig. 1(c), which shows the plots of corresponding total and non-condensate density profiles. Thus, a_{12} has to be greater than $295a_0$ at $T \neq 0$ for phase-separation to occur. To confirm that the suppression is a consequence of non-zero temperature, we identify and compute the number of condensate atoms in each species, and use these numbers for $T = 0$ computations. Despite the difference in the numbers of atoms, from the plots in Figs. 1(d-f), the TBEC retains the immiscible profiles at zero temperature. This implies that without the thermal cloud, there are no deviations from the usual phase-separation condition. For comparison, plots of n_{ck} from the finite temperature cases are also shown in the figure.

To investigate the spatial coherence at equilibrium, we examine the nature of the first order correlation function $g^{(1)}_k(z, z')$ as defined in Eq. (6). As to be expected, profile of $g^{(1)}_k(z, z')$ depends on the interplay between the interaction strength and temperature. As stated earlier, at $T = 0$, there is perfect coherence in the Cs-Rb TBEC and $g^{(1)}_{\text{Cs/Rb}}(0,z) = 1$ within the spatial extent of the condensates. This is independent of whether the TBEC is in miscible or immiscible regime.

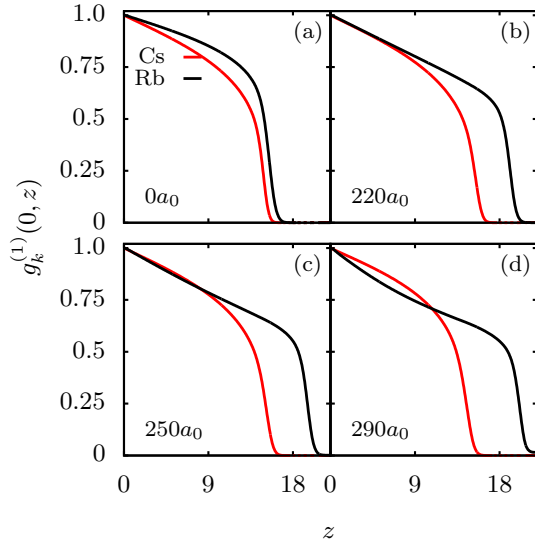FIG. 3. (Color online) (a)-(d) The first order spatial correlation function, $g^{(1)}_{\mathrm{Cs/Rb}}(0,z)$ with $z \geqslant 0$, of ^{87}Rb-^{133}Cs TBEC at equilibrium at $T = 5$nK for $a_{12} = 0, 220, 250, 290a_0$, respectively. Here z is measured in units of a_{osc}.
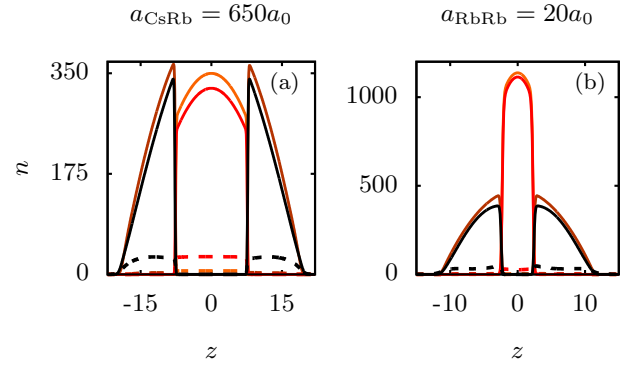

FIG. 4. (Color online) Density profiles showing complete phase-separation at $T = 0$ and $T = 10$nK. (a) Phase-separation in ^{87}Rb-^{133}Cs TBEC for $a_{12} = 650a_0$. The solid and dashed orange (brown) lines represent $n_{c\mathrm{Cs}}(n_{c\mathrm{Rb}})$ and $\tilde{n}_{c\mathrm{Cs}}(\tilde{n}_{c\mathrm{Rb}})$, respectively at $T = 0$. The solid and dashed red (black) lines represent $n_{c\mathrm{Cs}}(n_{c\mathrm{Rb}})$ and $\tilde{n}_{c\mathrm{Cs}}(\tilde{n}_{c\mathrm{Rb}})$, respectively at $T = 10$nK. (b) Phase-separation in ^{85}Rb-^{87}Rb TBEC for $a_{12} = 20a_0$. The solid and dashed orange (brown) lines represent n_c and $\tilde{n}$ of ^{85}Rb (^{87}Rb), respectively at $T = 0$. The solid and dashed red (black) lines represent n_c and $\tilde{n}$ of ^{85}Rb (^{87}Rb), respectively at $T = 10$nK. Here, n and z are measured in units of a_{osc}^{-1} and a_{osc}, respectively.

For simplicity and based on the symmetry of the system we consider $g^{(1)}_{\mathrm{Cs/Rb}}(0,z)$ with $z \geqslant 0$, and plots at different temperatures are shown in Fig. 2. At $T = 0$ the form of the $g^{(1)}_{\mathrm{Cs/Rb}}(0,z)$ remains unchanged as the system undergoes the dramatic transition from miscible to immiscible phase. This is evident from the plot in Fig. 2(a). However, when $T \neq 0$, unlike the zero temperature case, $g^{(1)}_{\mathrm{Cs/Rb}}(0,z)$ is maximum at $z = 0$ and decays to zero with z. This is due to the non-condensate atoms, which modify the the nature of coherence in the system. The rate of decay of the $g^{(1)}_{\mathrm{Cs/Rb}}(0,z)$ increases with temperature, and this is evident from the plots of $g^{(1)}_{\mathrm{Cs/Rb}}(0,z)$ at $T = 5$nK and $T = 10$nK shown in Figs. 2(b-c) for $a_{12} = 295a_0$. We also observe a dramatic variation in $g^{(1)}_{\mathrm{Cs/Rb}}(0,z)$ at fixed temperature, but the value of a_{12} is steered from miscible to immiscible regime. At the outset, when the TBEC is miscible at $a_{12} = 0$, $g^{(1)}_{\mathrm{Rb}}(0,z)$ decays to 0 at a larger distance than $g^{(1)}_{\mathrm{Cs}}(0,z)$ as shown in Fig. 3(a). This is because n_{Rb} has a larger spatial extent than n_{Cs}. As a_{12} is increased, the TBEC undergoes a phase-transition from miscible to sandwich type density profiles. Along with this, the distance at which $g^{(1)}_{\mathrm{Rb}}(0,z)$ falls off to zero increases with increase in a_{12}. On the contrary, the distance at which $g^{(1)}_{\mathrm{Cs}}(0,z)$ falls off to zero decreases with increase in a_{12}. This causes the $g^{(1)}_k(0,z)$ of the individual species to cross each other at a certain z_0. At z_0, the two species have equal $g^{(1)}_{\mathrm{Cs/Rb}}(0,z_0)$ and this is a characteristic signature of immiscible phase. These features are shown in Figs. 3(b-d). It deserves to be mentioned here that z_0 increases, and $g^{(1)}_{\mathrm{Cs/Rb}}(0,z_0)$ decreases with increase in a_{12}. In addition, there is a dramatic difference in the decay rates of $g^{(1)}_{\mathrm{Cs/Rb}}(0,z_0)$; it is much faster in Cs. This is

attributed to the fact that both $n_{c\mathrm{Rb}}$ and $\tilde{n}_{\mathrm{Rb}}$ increase along z within the bulk of Cs-Rb TBEC. Where as in Cs, around the origin $n_{c\mathrm{Cs}}$ decreases but $\tilde{n}_{\mathrm{Cs}}$ increases. This trend is similar with a single-species Cs condensate. The presence of Rb does not affect the nature of $g^{(1)}_{\mathrm{Cs}}(0,z)$ in Cs-Rb TBEC. Around the point of phase-separation $n_{c\mathrm{Rb}}(0)$ in a Cs-Rb TBEC is distinctly different from single species Rb condensate, so is the nature of $g^{(1)}_{\mathrm{Rb}}(0,z)$ [25].

Segregation independent of temperature — In the domain of large a_{12}, $U_{12} \gg \sqrt{U_{11}U_{22}}$, $\Lambda \approx 0$, and the phase-segregation is more prominent. However, due to the geometry of the TBEC mean-field approximation is still valid. In this domain the interfacial overlap is minimal and the TBECs assume sandwich type density profile. The system is then equivalent to three coupled condensate fragments, and as a result, the Bogoliubov analysis shows the presence of three Goldstone modes [28]. For the Cs-Rb TBEC considered here, the background inter-species scattering length $a_{\mathrm{CsRb}} = 650a_0$ satisfies the above condition. With this value of a_{12}, at $T = 0$ as shown in Fig. 4(a), Cs condensate lies at the center of the trap and Rb condensate at the edges. So, at the center $n_{\mathrm{Rb}}(0) = 0$ and $n_{\mathrm{Cs}}(0)$ is maximum. With the increase in a_{12}, there is a decrease in the number of non-condensate atoms arising from quantum fluctuations. This is a manifestation of smaller overlap between the condensates at the interfaces. On the contrary, for a single species BEC, with the increase in intra-species interaction strength, the number of non-condensate atoms due to quantum fluctuations increases[21]. When $T \neq 0$, the thermal density $\tilde{n}_k$ interact with the condensate clouds through the intra- and inter-species interactions. But, due to the large a_{12}, the inter-species interaction energy is much larger than the intra-species interaction energy. This makes $n_{\mathrm{Rb}}(0) \approx 0$, and there is little overlap of the thermal

cloud of one species with the condensate of the other species, such that $\Lambda < 0.1$. Thus, there is *no thermal suppression* in the the domain of large a_{12}. We observe similar results in the case of ^{85}Rb-^{87}Rb TBEC as well, where the the intra-species interaction of ^{85}Rb is decreased to obtain completely phase-separated density profiles. These are shown in Fig. 4(b).

Conclusions — At finite temperatures, to examine the properties of binary condensates in the neighbourhood of phase separation, it is essential to incorporate the thermal component. In general, there is a delay or suppression of phase-separation due to the thermal component, and we have examined this in detail with the Cs-Rb binary condensate as an example. In this system the transition is driven by tuning the inter-species interaction, and similar results are obtained in ^{85}Rb-^{87}Rb binary condensate, where tuning the intra-species interaction of ^{85}Rb induce the transition. The binary condensate mixtures of dilute atomic gases are different from the classical binary fluids which undergo miscible-immiscible transition with temperature as control parameter. First, the variation of temperature in TBECs is applicable only below the lower of the two critical temperatures. Second, each species has two sub-components, the condensate and non-condensate atoms. The condensate or the superfluid components are coherent, but the non-condensate components are incoherent and like the normal gas. Third, there are spatial

density variations of all the components due to the nature of the confining potential and diluteness of the atomic gas. Fourth, beyond a certain critical value of interaction strength or in the $U_{12} \gg \sqrt{U_{11}U_{22}}$ domain, temperature does not alter the density profiles. Finally, the transition to the phase separated domain at finite temperatures is associated with a distinct change in the profile of the correlation function. Our results provide an explanation of the experimentally observed density profiles at phase-separation[7]. Even when the phase-separation condition is satisfied there is a finite overlap between the two species at finite temperature which is due to the presence of thermal cloud. Our findings clearly demonstrate the dominance of thermal fluctuations over quantum fluctuations which causes the suppression of phase-segregation in any TBEC experiment.

[1] H. Stanley, *Introduction to Phase Transitions and Critical Phenomena*, International series of monographs on physics (Oxford University Press, 1971).
[2] S. Inouye, M. R. Andrews, J. Stenger, H.-J. Miesner, D. M. Stamper-Kurn, and W. Ketterle, Nature **392**, 151 (1998).
[3] C. Chin, R. Grimm, P. Julienne, and E. Tiesinga, Rev. Mod. Phys. **82**, 1225 (2010).
[4] G. Modugno, M. Modugno, F. Riboli, G. Roati, and M. Inguscio, Phys. Rev. Lett. **89**, 190404 (2002).
[5] G. Thalhammer, G. Barontini, L. De Sarlo, J. Catani, F. Minardi, and M. Inguscio, Phys. Rev. Lett. **100**, 210402 (2008).
[6] A. Lercher, T. Takekoshi, M. Debatin, B. Schuster, R. Rameshan, F. Ferlaino, R. Grimm, and H.-C. Nägerl, Euro. Phys. Jour. D **65**, 3 (2011).
[7] D. J. McCarron, H. W. Cho, D. L. Jenkin, M. P. Köppinger, and S. L. Cornish, Phys. Rev. A **84**, 011603 (2011).
[8] B. Pasquiou, A. Bayerle, S. M. Tzanova, S. Stellmer, J. Szczepkowski, M. Parigger, R. Grimm, and F. Schreck, Phys. Rev. A **88**, 023601 (2013).
[9] S. B. Papp, J. M. Pino, and C. E. Wieman, Phys. Rev. Lett. **101**, 040402 (2008).
[10] S. Tojo, Y. Taguchi, Y. Masuyama, T. Hayashi, H. Saito, and T. Hirano, Phys. Rev. A **82**, 033609 (2010).
[11] D. M. Stamper-Kurn, M. R. Andrews, A. P. Chikkatur, S. Inouye, H.-J. Miesner, J. Stenger, and W. Ketterle, Phys. Rev. Lett. **80**, 2027 (1998).
[12] J. Stenger, S. Inouye, D. M. Stamper-Kurn, H.-J. Miesner, A. P. Chikkatur, and W. Ketterle, Nature **396**, 345 (1998).
[13] C. J. Myatt, E. A. Burt, R. W. Ghrist, E. A. Cornell, and C. E. Wieman, Phys. Rev. Lett. **78**, 586 (1997).
[14] L. E. Sadler, J. M. Higbie, S. R. Leslie, M. Vengalattore, and D. M. Stamper-Kurn, Nature **443**, 312 (2006).
[15] C. Pethick and H. Smith, *Bose-Einstein Condensation in Dilute Gases* (Cambridge University Press, New York, 2008).
[16] B. V. Schaeybroeck, Physica A **392**, 3806 (2013).
[17] C.-C. Chien, F. Cooper, and E. Timmermans, Phys. Rev. A **86**, 023634 (2012).
[18] H. Shi, W.-M. Zheng, and S.-T. Chui, Phys. Rev. A **61**, 063613 (2000).
[19] A. Griffin, Phys. Rev. B **53**, 9341 (1996).
[20] N. M. Hugenholtz and D. Pines, Phys. Rev. **116**, 489 (1959).
[21] A. Roy and D. Angom, Phys. Rev. A **90**, 023612 (2014).
[22] F. Wang, D. Xiong, X. Li, D. Wang, and E. Tiemann, Phys. Rev. A **87**, 050702 (2013).
[23] A. Simoni, F. Ferlaino, G. Roati, G. Modugno, and M. Inguscio, Phys. Rev. Lett. **90**, 163202 (2003).
[24] K. Pilch, A. D. Lange, A. Prantner, G. Kerner, F. Ferlaino, H.-C. Nägerl, and R. Grimm, Phys. Rev. A **79**, 042718 (2009).
[25] See supplementary material for details.
[26] S. L. Cornish, N. R. Claussen, J. L. Roberts, E. A. Cornell, and C. E. Wieman, Phys. Rev. Lett. **85**, 1795 (2000).
[27] J. L. Roberts, N. R. Claussen, J. P. Burke, C. H. Greene, E. A. Cornell, and C. E. Wieman, Phys. Rev. Lett. **81**, 5109 (1998).
[28] A. Roy, S. Gautam, and D. Angom, Phys. Rev. A **89**, 013617 (2014).
[29] P. Jain and M. Boninsegni, Phys. Rev. A **83**, 023602 (2011).
[30] D. S. Petrov, G. V. Shlyapnikov, and J. T. M. Walraven, Phys. Rev. Lett. **85**, 3745 (2000).
[31] S. De, D. L. Campbell, R. M. Price, A. Putra, B. M. Anderson, and I. B. Spielman, Phys. Rev. A **89**, 033631 (2014).
[32] B. Van Schaeybroeck, Phys. Rev. A **78**, 023624 (2008).